Atmospheric
Chemistry
and Physics
Discussions

Impacts of seasonal and regional variability in biogenic VOC emissions on surface ozone in the Pearl River Delta region, China

S. Situ[1], A. Guenther[2], X. Wang[1], X. Jiang[2], A. Turnipseed[2], Z. Wu[1], G. Zhou[3], J. Bai[4], and X. Wang[5]

[1]School of Environmental Science and Engineering, Sun Yat-sen University, Guangzhou 510275, China
[2]National Center for Atmospheric Research, CO, USA
[3]South China Institute of Botany, Chinese Academy of Sciences, Guangzhou 510650, China
[4]LAGEO, Institute of Atmospheric Physics, Chinese Academy of Sciences, Beijing, China
[5]Institute of Geochemistry Chinese Academy of Science, Guangzhou 510650, China

Correspondence to: X. Wang (eeswxm@mail.sysu.edu.cn)

Abstract

In this study, the BVOC emissions in November 2010 over the Pearl River Delta (PRD) region in southern China have been estimated by the latest version of a Biogenic Volatile Organic Compound (BVOC) emission model (MEGAN v2.1). The evaluation of
5 MEGAN performance at a representative forest site within this region indicates MEGAN can estimate BVOC emissions reasonably well in this region except overestimating isoprene emission in autumn for reasons that are discussed in this manuscript. Along with the output from MEGAN, the Weather Research and Forecasting model with chemistry (WRF-Chem) is used to estimate the impacts of BVOC emissions on surface ozone in
10 the PRD region. The results show BVOC emissions increase the daytime ozone peak by ∼ 3 ppb on average, and the max hourly impacts of BVOC emissions on the daytime ozone peak is 24.8 ppb. Surface ozone mixing ratios in the central area of Guangzhou-Foshan and the western Jiangmen are most sensitive to BVOC emissions BVOCs from outside and central PRD influence the central area of Guangzhou-Foshan and
15 the western Jiangmen significantly while BVOCs from rural PRD mainly influence the western Jiangmen. The impacts of BVOC emissions on surface ozone differ in different PRD cities, and the impact varies in different seasons. Foshan and Jiangmen being most affected in autumn, result in 6.0 ppb and 5.5 ppb increases in surface ozone concentrations, while Guangzhou and Huizhou become more affected in summer. Three
20 additional experiments concerning the sensitivity of surface ozone to MEGAN input variables show that surface ozone is more sensitive to landcover change, followed by emission factors and meteorology.

1 Introduction

Formed by photochemical reactions involving volatile organic compounds (VOCs) and
25 the oxides of nitrogen ($NO_x = NO + NO_2$) (Chameides et al., 1992), surface ozone is the most abundant atmospheric photochemical oxidant and can adversely affect human

health, vegetation and welfare (Viney et al., 1992). VOCs can originate either from anthropogenic or biogenic sources. Globally speaking, biogenic VOC (BVOC) emissions are much higher than anthropogenic VOC emissions, accounting for 90 % of total atmospheric VOC emissions (Guenther et al., 1995). Measurement and modeling of BVOCs are essential for understanding regional and global atmospheric chemistry, carbon cycle and climate change.

Over the past few decades, research has been conducted to measure emissions of carbon-containing compounds from vegetation and hundreds of BVOCs have been identified. At the present time, BVOC studies focus on four aspects: (1) understanding the mechanisms controlling BVOC emissions; (2) improving and applying BVOC measurement technology; (3) developing and improving BVOC emission models and estimating the emissions; and (4) quantifying the atmospheric chemistry impacts of BVOC emissions (Guenther et al., 1995, 1996a,b, 1999, 2006, 2012; Carslaw et al., 2000; Wang et al., 2011). Most BVOCs quickly react with OH and then influence atmospheric composition, especially ozone and secondary organic aerosol (Carslaw et al., 2000; Hoffman et al., 1997), by a series of chemical actions. The impacts of BVOCs on global chemistry have been investigated using global models (Granier et al., 2000; Poisson et al., 2000; Collins et al., 2002; Sanderson et al., 2003), and the results show that BVOCs can affect global chemistry significantly. High-resolution studies on regional and local scales also show that the impacts of BVOC emissions on air quality are very important (Thunis et al., 2000; Fabien et al., 2004; Li et al., 2007; Curci et al., 2009; Bao et al., 2010; Marley et al., 2009; Geng et al., 2011; Fu et al., 2012; Wei et al., 2007). It has also been shown that the results are very useful for developing pollution control strategies (Pierce et al., 1998).

Located in the central Guangdong province in southern China, the Pearl River Delta (PRD) region is one of the most developed areas in China. Nine major cities in the PRD region form a super-city cluster, including Guangzhou (GZ), Dongguan (DG), Foshan (FS), Shenzhen (SZ), Zhuhai (ZH), Zhongshan (ZS), Jiangmen (JM), Huizhou (HZ), and Zhaoqing (ZQ). Because of its geographic location, the PRD region is influenced

Title Page

Abstract | Introduction

Conclusions | References

Tables | Figures

◄◄ | ►►|

◄ | ►

Back | Close

Full Screen / Esc

Printer-friendly Version

Interactive Discussion

by a subtropical monsoon climate, having the characteristics of high temperature and high humidity in most seasons. Vegetation in this region is mainly subtropical evergreen forest and some of the species such as eucalyptus have very high BVOC emission capacities (Klinger et al., 2002). These features enhance BVOC emissions in the PRD region. Emission inventory studies have suggested that the BVOC emissions in the PRD are very high and the annual average isoprene emission flux is higher than Beijing, China, and the averaged value over North America (Zheng et al., 2010b; Wang et al., 2011).

Because of the remarkable economic development and rapid urban expansion, air quality in the PRD has been deteriorating in recent years. Ozone and particle matter are the major air pollutants in this region, with the maximum hourly average ozone concentration exceeding 180 ppb in 2008 (the national standard is 100 ppb in China). Society and government are concerned about this issue, and a series of studies have been carried out to provide an in-depth understanding and a comprehensive record, including concentration measurement and analysis (Zhang et al., 2008; Zheng et al., 2010a), the relationship between ozone and its precursors (Cheng et al., 2010; Wang et al., 2010a), the meteorological analysis of a season with high ozone concentration (Fan et al., 2008) and the impacts of anthropogenic emissions on ozone formation (Wang et al., 2005; Li et al., 2011). Recently, some studies showed that BVOCs emissions could affect surface ozone in the PRD region. Tang et al. (2007) investigated VOCs at urban, suburban, and rural sites in the PRD, and found that biogenic isoprene emission contributed significantly to the ozone formation potential especially at a remote site. However, this study only focused on VOCs concentration and their ozone formation potential and did not quantify how BVOC emissions affect surface ozone spatiotemporally. Wei et al. (2007) used an atmospheric chemical model to study the impacts of BVOCs on an ozone episode during a tropical storm in the PRD, and the results indicated that BVOCs could increase the daytime ozone peak up to 15.2 ppb. However, this study only focused on a specific period and there was no systematic and quantitative evaluation of the importance of BVOCs on regional ozone formation.

Seasonal and regional variability in biogenic VOC emissions

S. Situ et al.

Title Page

Abstract	Introduction
Conclusions	References
Tables	Figures

◄◄   ►►

◄   ►

Back   Close

Full Screen / Esc

Printer-friendly Version

Interactive Discussion

Overall, it is not well understood and needs to be addressed in BVOCs emissions affecting surface ozone over the PRD region.

The objectives of this paper are to: (1) evaluate MEGAN performance in a typical subtropical area in South China and (2) study the impacts of BVOC emissions on surface ozone in this area. In this study, we used the Model of Emissions of Gases and Aerosols from Nature version 2.1 (MEGAN2.1) to estimate BVOC emissions in the PRD region at a high spatiotemporal resolution and applied them in a fully coupled weather-chemistry model (WRF-Chem) to study the impacts of seasonal and spatial variability in BVOC emissions on surface ozone. The paper is organized as follows. In Sect. 2 and Sect. 3, the modeling and measurement approaches are described, respectively. Result and discussion, including the model performances and impacts of BVOC emissions on the surface ozone, are presented in Sect. 4, which is followed by the conclusions in Sect. 5.

2 Modeling approach

2.1 WRF-Chem description

The model used in this study is the chemistry version of the WRF model (WRF-Chem v3.2.1). The WRF model is a mesoscale non-hydrostatic meteorological model that includes several options for physical parameterizations of the Planetary Boundary Layer (PBL), cloud processes and land surface (Skamarock et al., 2008). The chemistry version is a version of WRF coupled with an "online" chemistry model, in which meteorological and chemical components of the model are predicted simultaneously (Grell et al., 2005; Fast et al., 2006).

Three domains (d01, d02, and d03) were adopted in this study, and the spatial resolutions of these three domains were 27, 9 and 3 km respectively (Fig. 1). The chemistry calculation was only applied in d03. To reduce the biases in modeled meteorology, analysis nudging was used in d01 (Deng et al., 2007). The NCEP 1° × 1° reanalysis data

were used as initial and boundary conditions for meteorology. There were 24 sigma vertical layers extending from surface to 100 hPa and 10 vertical layers were set in the PBL. Main options for physical and chemical schemes adopted in this study are listed in Table 1 (Chen and Dudhia, 2001; Martilli et al., 2002; Janjic et al., 2002; Kain et al., 1990, 1993; Lin et al., 1983; Chou et al., 1998; Mlawer et al., 1997). The Kain–Fritsch cumulus parameterization scheme was used in the d01 and d02, and no cumulus parameterization scheme was used for the finest domain (d03) in this study because the convection is assumed to be reasonably well characterized by the explicit microphysics (Wang et al., 2007).

The gas phase chemistry scheme CBM-Z (Zaveri and Peters, 1999) and the MOSAIC aerosol model (Zaveri et al., 2008) were selected as the chemical mechanisms for this study because they can better represent surface ozone that agrees with the observations in the PRD region (Wang et al., 2009). CBM-Z is a new lumped structure photochemical mechanism for large-scale applications. It extends the original CBM-IV framework to function properly at larger spatial and longer timescales. It includes 52 chemical species and 132 photolytic gas phase reactions, of which 7 reactions are isoprene chemical reactions. MOSAIC is a Model for Simulating Aerosol Interactions and Chemistry, which can treat all the important aerosol species at urban, regional and global scales (Zeverl et al., 2008). MOSAIC is implemented in the sectional framework to represent the aerosol size distribution where the aerosol size distribution is divided into discrete size bins. Each bin is assumed to be internally mixed so that all particles within a bin have the same chemical composition, and water uptake or loss does not transfer particles between bins. In the version used in this study, secondary organic aerosols (SOA) were not included.

It should be noted that monoterpenes are not treated as a unique species in the CBM-Z chemical scheme. Instead, we accounted for terpene species (e.g. α-pinene and β-pinene) by lumping them into the CBM-Z OLEI (internal olefin carbons) and OLET (terminal olefin carbon) categories for this study. The reaction rate constant with OH for OLEI (OLET) in WRF-Chem has been compared with the measured values for

Title Page

Abstract | Introduction

Conclusions | References

Tables | Figures

◄ | ►►

◄ | ►

Back | Close

Full Screen / Esc

Printer-friendly Version

Interactive Discussion

some individual monoterpene species (e.g. α-pinene, β-pinene and limonene). The comparison indicates that the reaction rate constants with OH for OLEI is very close to the measured value (α-pinene) while the reaction rate constant with OH for OLET is lower than the measured values for the monoterpenes lumped into this category (e.g.

5 β-pinene and limonene) (Atkinson et al., 2003). OLEI includes not only the biogenic internal alkenes, but also the anthropogenic internal alkenes which are emitted in greater magnitude than biogenic internal alkenes. Moreover, the contribution of terpenes to ozone formation is lower than isoprene even when terpene chemistry is treated individually (Curci et al., 2009). As a result, the use of the model default reaction rate constant

10 with OH for OLEI for monoterpenes should be a reasonable approach to get the relative contribution of monoterpene emissions to the surface ozone over the PRD region in this study.

2.2 Anthropogenic emissions

A highly resolved temporal and spatial PRD regional emission inventory for the year
15 2006 was developed with the use of best available domestic emission factors and activity data (Zheng et al., 2009). A bottom-up approach was adopted to compile the inventory for major emission sources, including industry, mobile, resident and biogenic sources. The results included the annual emission amount for sulfur dioxide, nitric oxide, carbon monoxide, VOCs and particles.
20 The regional emission inventory was updated to 2010, and the spatial distributions are shown in Fig. 2a–d.The spatial pattern of sulfur dioxide emission agrees well with industrial centers, while those of nitric oxide, carbon monoxide and VOCs emissions agree well with vehicle emissions and industry.

2.3 Biogenic emissions

25 MEGAN is the new generation model of emissions of gases and aerosols from nature which has been widely used to estimate the global and regional BVOC emissions

(Guenther et al., 2006; Sakulyanontvittaya et al., 2008; Wang et al., 2011; Geng et al., 2011). The recently developed MEGAN v2.1 is used to estimate BVOC emissions in this study. The above canopy meteorology drives the microscale meteorology inside a plant canopy which can directly affect BVOC emissions. A multi-layer explicit canopy model incorporated into MEGAN v2.1 calculates the canopy microscale meteorology, including the temperature and radiation flux on sun and shaded leaves, by accounting for the radiation transmission and energy balance. MEGAN v2.1 can estimate emissions of up to 146 BVOC species and output them as individual compounds or as the inputs required for specific atmospheric chemistry mechanisms (Guenther et al., 2012).

Meteorology, Plant Functional Types (PFTs), Leaf Area Index (LAI) and emission factors (EFs) are the inputs required to drive MEGAN. Different from the PFTs used in the previous version, MEGAN v2.04 (Sakulyanontvittaya et al., 2008), 16 plant function types are considered in MEGAN v2.1, including arctic, boreal, temperate, and tropical plants, C3 and C4 grasses, and evergreen and deciduous shrubs (Bonan et al., 2002; Olesonet al., 2000). Moreover, high-resolution 8-day LAI can be used in MEGAN v2.1 in order to better capture the temporal variation of vegetation. In this study, the PFTs and LAI data were the same as those used by Wang et al. (2011). The meteorology data were simulated by WRF-Chem. Emission factors of BVOCs were calculated based on the literature recommendations in the PRD region (Bai et al., 2001a,b; Klinger et al., 2002; Tsui et al., 2009).

Total BVOCs, including isoprene, monoterpene, sesquiterpene and other compounds (e.g. acids, aldehyde, alcohols and some other volatile compounds), are included in WRF-Chem simulations conducted for this study. Figure 2e shows the total BVOC emission flux in d02, and it indicates that there are considerable spatial variations in the total BVOC emissions over d03 which can be divided into three regions: the outside PRD, the rural PRD and the central PRD (Fig. 1). The outside PRD is the area inside the modeling domain but outside the PRD region. The rural PRD represents the rural and less developed areas in the PRD region, including Huizhou, north and northeast of Guangzhou, west of Foshan, Jiangmen and Zhaoqing. Excluding the

rural PRD, the remaining PRD region is defined as the central PRD in this study. The amounts of BVOC emissions from the three regions contribute to 68.4 %, 26.2 % and 5.4 % of the total BVOC emissions from the whole domain, respectively. The MEGAN result also indicates that isoprene emissions dominated total BVOC emissions in day-time, accounting for ∼ 60 % of total BVOC emissions.

2.4 Experimental design

To thoroughly evaluate the impacts of BVOC emissions on surface ozone over the PRD region, annual ensemble simulations are preferred. However, annual ensemble simulations with this fully coupled atmosphere-chemistry model demand a huge amount of computing time. The alternative approach used for this study is to select the highest ozone month as the simulated period to minimize computer resource requirements and investigate the effects under high ozone concentration, which is typically of greatest interest for the air quality regulatory community.

Multiple years of observations show that high ozone concentrations frequently occurred in autumn in the PRD (Zheng et al., 2010a) because of the high frequency of a surface high-pressure system and the descent motion outside of hurricane and sea breeze in this season (Fan et al., 2008). Meanwhile, we initiated BVOC emission flux measurements in Dinghu Mountain in the PRD in November 2010 using the Relaxed Eddy Accumulation (REA) technique, and the results were used to evaluate the MEGAN model. Thus, November 2010 was chosen for the simulated period to investigate the role of BVOCs in a period of high ozone.

General weather conditions over the PRD in November 2010 favored ozone formation with a surface high-pressure and northerly wind yielding scattered showers and the sky was generally clear. Three northerly cold air masses entered the PRD region on 8, 15 and 22 November, and caused an increase of wind speed and decrease of temperature (http://www.tqyb.com.cn/index.asp). General conditions including surface pressure, temperature, wind speed and relative humidity are listed in Table 2.

One month long simulation using anthropogenic emissions and total BVOC emissions was conducted as the control run for this study. In addition, 5 experiments with different chemical emission scenarios were designed (Table 3) to study the impacts of BVOC emissions on surface ozone. Excluding anthropogenic emissions, case 1 was designed to estimate the impacts of BVOC emissions on surface ozone in a clean atmosphere, which could indicate the background value of surface ozone due to BVOC emissions in this region. In case 2, the BVOC emissions were removed in order to quantify the impacts of BVOC emissions on surface ozone in the real atmospheric environment. As isoprene is emitted into the troposphere in greater quantities than other non-methane BVOCs and it is very reactive in the atmosphere, case 3 was designed to estimate the impacts of isoprene emissions on surface ozone. Case 4 and case 5 were designed to study the regional impacts by excluding the BVOC emissions from the outside PRD and the rural PRD. Case 6 was a seasonal comparison simulation to estimate the impacts of BVOC emissions in summer in this region. Aerosol feedback turned off in all cases in order keep the same meteorology.

3 Measurement approach

In autumn 2010, a field experiment was conducted at Dinghu Mountain, using the REA technique to quantify BVOC emission fluxes from a typical natural forest in this region. As far as we know, this is the first whole canopy BVOC flux measurement made in the PRD region. The measurements were made on a 37 m high canopy flux tower operated by the South China Botanical Garden of the Chinese Academy of Sciences in Dinghu Mountain (112.53° E 23.17° N) in the northwest of PRD, which is 86 km away from Guangzhou. The REA system was installed at a height of 31 m above ground and more than 10 m above the forest canopy (canopy height is around 17 m). This site is mainly covered by subtropical evergreen broadleaf forest, with some needleleaf conifers, and most trees are more than 100 yr old. Details about the site description can be found in Zhou et al. (2007).

The theory behind REA has been explained elsewhere (Businger et al., 1990; Bowling et al., 1998). In short, two air samples are collected over a statistically meaningful time period (~ 30 min); one consisting of updrafts and the other consisting of downdrafts. While alternating sampling between the up and down reservoirs, depending on the vertical wind direction, the flow occurs at a constant flow rate. The duration of sample collection for each reservoir is related to the frequency at which the wind eddies change vertical direction (Baker et al., 2001). The flux calculation can be described as followed:

$$F = \beta \sigma_w (C_u - C_d) \tag{1}$$

Where β is a dimensionless coefficient which is determined empirically from fast response temperature measurements, σ_w is the standard deviation of the vertical wind over the collection period and C_u and C_d are measured concentrations collected in the updraft and downdraft reservoirs.

All samples were collected on Tenax TA and Carbograph 5TD solid adsorbent cartridges and shipped to the lab at NCAR (National Center for Atmospheric Reach, Boulder, CO, USA) for chemical analysis by Gas Chromatography. Cartridges were desorbed using an Ultra auto sampler with a Unity thermal desorption system (MARKES International, Llantrisant, UK) coupled to a 7890A series Gas Chromatograph with a 5975C Electron Impact Mass Spectrometer and flame ionization detector (GC-MS/FID, Agilent Technologies, Santa Clara, CA, USA). VOCs were separated with an Agilent HP-5 ms column (Agilent Technologies, USA) using an initial oven temperature of $35\,°C$ for 1 min followed by a temperature ramp of $6\,°C\,min^{-1}$ to $80\,°C$, then $3\,°C\,min^{-1}$ to $155\,°C$, then $10\,°C\,min^{-1}$ to $190\,°C$, and finally $25\,°C\,min^{-1}$ to $260\,°C$ with a 5 min final hold. Helium was used as a carrier gas, at a flow rate of $3\,mL\,min^{-1}$. Concentrations were quantified using FID calibrated with a NIST traceable standard. Compounds with co-eluting peaks were quantified with the MS using specific masses that were normalized by the same or similar mass in the internal standards (tetramethylethene and dihydronapthalene) that were introduced for each run using a 1 mL loop. Identifications

were mostly based on comparison of retention times and mass spectra of authentic standards but in a few cases were based on the retention times and mass spectra in the Adams et al. (2001) and NIST databases.

4 Result and discussion

4.1 Model performance

4.1.1 Meteorology

Available daily averaged data observed at 9 weather stations (including Fogang, Guangning, Gaoyao, Guangzhou, Dongyuan, Zengcheng, Huiyang, Taishan and Shenzhen) for November 2010 were used to validate the simulated 2-m temperature, 10-m wind speed, and 2-m relative humidity from the control run. The simulated downward shortwave radiation was validated by the hourly downward solar radiation observed in Dinghu. The statistics of the verification, including the bias, mean absolute errors (MAE) and root mean square errors (RMSE) are listed in Table 4.

The result shows that the simulated downward shortwave radiation is higher than the observation. This may at least partly be due to the fact that the model did not include aerosol feedback in this study. Because of the simulated higher downward shortwave radiation, modeled 2-m temperature has a warm bias of 1.2° and 2-m relative humidity has a dry bias of -2.1%. The simulated 10-m wind speed is $2.2\,\mathrm{m\,s^{-1}}$ higher than the observation which is expected since WRF generally overestimates wind speed in a flat area (Roux et al., 2009; Mass et al., 2010, 2011). Overall, the meteorological conditions simulated by the model are reasonable.

4.1.2 BVOC emissions

The analysis of REA samples shows that the main BVOCs emitted from the Dinghu Mountain forest include isoprene, α-pinene, β-pinene, camphene and D-limonene.

After excluding fluxes that did not meet required conditions, isoprene emission fluxes range between 0.002 and 0.215 mg m^{-2} h^{-1} and monoterpene emission fluxes range between 0.063 and 0.313 mg m^{-2} h^{-1} on mid-day in autumn 2010.

The landcover inputs used to parameterize the Dinghu site in MEGAN include an LAI value of 3 for November and a PFT composition of 42.3 % broadleaf trees and 20.9 % needleleaf trees. Along with the local measurements of BVOC emission factors for dominate tree species at this site, the contributions of trees species in the PRD to the total tree cover of the area were used to weight and group the EFs for each PFT. Monitored meteorological data at the Dinghu site were used to drive MEGAN. Model results show that the isoprene emission rates vary from 0.366 to 3.577 mg m^{-2} h^{-1} and monoterpene emission rates are between 0.149 and 0.617 mg m^{-2} h^{-1} on mid-day during the REA sampling period. Compared to the REA observations, MEGAN agrees well with monoterpene emission flux, but considerably overestimates the isoprene emission flux.

This initial study of above canopy fluxes in the PRD region indicates that isoprene emissions can be very different from the model estimate. However, there are very high uncertainties in modeled isoprene estimates for almost all vegetation types (Zheng et al., 2010b), so we used stainless steel canister concentration measurements to further evaluate the MEGAN performance.

To compare the emission flux from MEGAN and the concentration from stainless steel canister samples, a simple box model was used to convert the modeled MEGAN isoprene emission flux to mixed layer concentration. Details about this simple box model have been described by Guenther et al. (1996b), and the equation can be written as:

Full Screen / Esc

Printer-friendly Version

Interactive Discussion

$$C = \frac{EF}{Z_i L} \qquad (2)$$

Where C is the mean scalar mixing ratio; EF is the emission flux; Z_i (m) is the height of mixed-layer capping inversion; L (s^{-1}) the oxidation rate of hydrocarbons. In this simple box model, only OH and O_3 are considered to oxidize hydrocarbons. So L is defined as $[k_{OH}OH] + [k_{O_3}O_3]$, where k_{OH} and k_{O_3} are reaction rate constants and OH and O_3 are mixing ratios of hydroxyl radical and ozone, respectively. To estimate the chemical loss, we used the OH and ozone reaction rate coefficients reported by Atkinson et al. (2003) and the measured ozone mixing ratios at Dinghu Mountain. No measured OH concentration data are available at this site, so the max OH concentration in the PRD on a summer day (Lu et al., 2012) was applied in this calculation. The result shows that isoprene concentrations based on MEGAN range between 0.1 to 1.3 ppb for a mid-day average in autumn, which agrees with the measured isoprene concentration ($\sim$ 0.1 ppb) in 2008 at Dinghu Mountain. The modeled isoprene concentration is 2.2 ppb for mid-day average in summer, which agrees well with the measured isoprene concentration in summer at Dinghu Mountain (Bai et al., 2001b).

In conclusion, the evaluation indicates that monoterpene emission fluxes estimated by MEGAN agree well with the observation at the Dinghu site, but isoprene is overestimated in autumn while it agrees well with the measurement in summer. The possible reasons for the overestimated isoprene emission flux by MEGAN include:

1. The MEGAN emission algorithms for characterizing seasonal variations are based on measurements in temperate landscapes (Monson et al., 1994; Petron et al., 2001) and may not account for seasonal variations in isoprene emissions at tropical or subtropical sites (Barkley et al., 2009).

2. There are few isoprene emission factor measurements reported in the literature for this region, and the available data for a given species are sometimes conflicting indicating large uncertainties in these emission factors.

3. MEGAN uses the past 24 h to normalize the emission factors under standard conditions and some special weather phenomena may not be considered. Thus, a longer normalization may be needed to fully account for the environmental influence.

Therefore, more field experiments are needed to accurately quantify the BVOC emission flux in the PRD region. This will provide a more in-depth understanding of the BVOC emission fluxes in this region and further improve the MEGAN model.

4.1.3 Surface ozone

Available hourly observed data at 4 monitoring sites (including WQS, LH, JGW and CZ) for November were used to validate the ozone simulation from the control run. The locations of these 4 monitoring sites are shown in Fig. 1. The site WQS is located 30–50 km downwind of the central Guangzhou-Dongguan-Foshan metropolitan urban areas and represents a regional scale site. The site LH is in the central Guangzhou, which is a typical urban site. The site JGW is in Huizhou, which is chosen as a rural or less developed area site in the eastern PRD. The site CZ in Zhaoqing is representative of rural or less developed areas in western PRD. The four sites represent the main areas in the PRD and will be used to illustrate the impacts of BVOCs on surface ozone in the different areas of the PRD.

Figure 3 shows that the control run reproduced the diurnal variations and magnitude of ozone reasonably well at most sites. As an important precursor of ozone, the comparison of NO_2 at the monitoring sites further demonstrates that the ozone formation is captured reasonably well over the domain throughout the period. Model appeared to underestimate ozone at LH, especially at night. This might be related to a combination of several factors, such as the uncertainties in the precursor emissions, meteorological parameters and chemical mechanism (Wang et al., 2010). Considering the prevailing northerly winds in November, the underestimation of ozone at LH might be caused mainly by the uncertainties in emissions in northern rural areas of Guangzhou and

Title Page

Abstract | Introduction

Conclusions | References

Tables | Figures

◄ | ►

◄ | ►

Back | Close

Full Screen / Esc

Printer-friendly Version

Interactive Discussion

distant northern areas outside of Guangzhou, such as Qingyuan. The overestimation of surface wind speeds might result in more transport and less accumulation of ozone and its precursors, and this was probably another important contributor to the underestimated ozone at LH. Moreover, the nighttime vertical diffusion is not easily simulated by current mesoscale meteorological models, especially over the complex topography and land use in PRD (Wang et al., 2010).

Surface ozone concentration increases significantly and has a large spatiotemporal variation over the PRD. The highest ozone concentration occurs at 15:00:00 LT, with a regional averaged value of ∼ 50 ppb (Fig. 4), and the ozone concentration is higher in the western PRD and the south of central PRD, because of the northeast prevailing wind direction (Fig. 5a).

4.2 Background influence of BVOC emissions on surface ozone

By excluding all anthropogenic emissions, the background level of surface ozone due to BVOC emissions over the PRD region was estimated. The daily average background ozone concentration is ∼ 25 ppb. This result also shows the small temporal variability of surface ozone in the background, varying from 22–29 ppb in daytime, and the maximum occurs at 15:00:00 LT valued 28.2 ppb. The spatial distribution of surface ozone at 15:00:00 LT showed in Fig. 5b, and it indicates that the spatial distribution is relatively smooth over of the PRD region.

The simulated background level of surface ozone indicates that BVOC emissions alone do not result in an ozone problem. The high level of ozone concentration is a result of the influence of anthropogenic pollutants emitted into the atmosphere. However, BVOC emissions must be considered when examining anthropogenic emission control strategies, because the ratio of ozone precursors (i.e. VOCs and NO_x) may change and then affect the formation of ozone and some secondary atmospheric pollutants.

4.3 Impacts of BVOC emissions on surface ozone

There is distinct difference between surface ozone simulations with and without BVOC emissions (Fig. 4). The difference rises together with BVOC emissions in the morning, and reaches the peak value of 3.0 ppb at 14:00:00 LT. The difference remains at
5 high value until 17:00:00 LT, and then begins to fall. This phenomenon indicates BVOC emissions generate additional surface ozone and contribute ∼ 3.0 ppb to the daytime ozone peak in this region. And the impact remains in this region and keep high value for approximately 3 h in the afternoon. As the most abundant non-methane BVOC, isoprene contributes ∼ 57 % to the impacts of total BVOC emissions on the daytime ozone
10 peak in the PRD.

Besides, the averaged impacts of BVOC emissions on surface ozone are obtained at each grid at 15:00:00 LT, when the regional ozone peak appears. The result indicates the central area of Guangzhou-Foshan and the western Jiangmen are where surface ozone is most sensitive to BVOC emissions (Fig. 6a), and the BVOC emissions can
15 increase the daytime ozone peak by 7.9 and 9.4 ppb averagely in these two places. In order to know the upper limit of BVOC emissions affecting the daytime ozone peak over the PRD region, the hourly maximum impacts of BVOC emissions on surface ozone are obtained at each grid at every 15:00:00 LT as well (Fig. 7a). It indicates that the impact of BVOC emissions on the daytime ozone peak can be as high as 24.8 ppb in the PRD
20 region, and it varies between 10 to 24.8 ppb in the central area of Guangzhou-Foshan and the western Jiangmen. Located in the central PRD, the central area of Guangzhou-Foshan is a major urban center/government area in the PRD region, where it is urgent to control the ozone pollution.

Figure 8 shows the impacts of BVOC emissions on surface ozone at 4 air quality
25 monitoring sites. The BVOC emissions at JGW are the highest, 10 times higher than at LH, but the impacts on surface ozone at JGW are the least significant (less than 2 ppb), and the diurnal variation of surface ozone increment due to BVOC emissions is very smooth at this site. This is mainly because (1) low NO_x does not favor ozone formation

because it is NO_x-limit at the JGW site (Zhang et al., 2008; Wang et al., 2010); and (2) the upwind location is not impacted by ozone accumulation. Even though the BVOC emissions are lower than $4\,mol\,km^{-2}\,h^{-1}$ at LH, the contribution of BVOC emissions to surface ozone is the highest, more than 4 ppb. The impacts of BVOCs on surface ozone at WQS and CZ are very similar at noon, ranging from 2 to 4 ppb. The impacts at CZ reach the maximum at 18:00:00 LT, which can be attributed to the influence of ozone transport, because CZ is on the downwind edge of PRD in November. This comparison also indicates that BVOC emissions have a higher impact on surface ozone in urban areas than in rural or less developed areas in the PRD region.

Figure 7a also suggests that there is a strong day-to-day difference of the impact of BVOC emissions on the daytime ozone peak over the PRD region, depending on the daily variation of meteorology, especially the wind speed and wind direction. With surface wind analysis performed over the PRD region, 3 distinct impact conditions are classified: north wind condition; calm wind condition; and south wind condition. The occurrence probabilities of the three conditions are 60.0 %, 36.7 % and 3.3 %, respectively. The BVOC impact patterns are quite different for the three conditions (Fig. 9). South wind condition is a rare condition, and it happens when the PRD region is controlled by a high ridge that is located to the east of the PRD. During south wind condition, BVOC emissions affect the daytime ozone peak more in the rural or less developed areas, including the northeast of Zhaoqing, north of Guangzhou, north of Jiangmen, and east of Dongguan, and it causes an average 2.8 ppb ozone increment over the PRD. North wind condition, the most common condition during the simulation, results in impacts of BVOC emissions on the daytime ozone peak of about 1.1 ppb increment in the PRD region on average and the surface ozone increases more in the central area of Guangzhou-Foshan and the western Jiangmen. Calm wind is conducive to ozone accumulation and it is easy to cause high ozone concentrations that can lead to an ozone pollution episode. During calm wind condition, BVOC emissions can increase the daytime ozone peak in much of the PRD region, and the increment is 2.1 ppb over the PRD region averagely.

4.4 Regional variability

The impacts of BVOC emissions from outside, central and rural PRD have been esti-
mated, and the results are shown in Fig. 6b–d. The influence of BVOC emissions from
the outside PRD is very similar to that of the BVOC emissions from the whole domain
(Fig. 6a, b), and the central area of Guangzhou-Foshan and northwestern Jiangmen
are, again, where the surface ozone is most sensitive to BVOC emissions. The BVOCs
from the central PRD affect the central area of Guangzhou-Foshan (Fig. 6d). We can
conclude that surface ozone in the central area of Guangzhou-Foshan is more sensi-
tive to the BVOC emissions from outside and central PRD. In contrast, the BVOCs from
the rural PRD affect the ozone mainly in northwestern Jiangmen (Fig. 6c).

The impacts of BVOC emissions on surface ozone are different in various PRD cities
(Fig. 10), which can be explained by (1) the amount of BVOCs emission; (2) the relative
location of emission sources; and (3) the meteorological conditions, including horizon-
tal transport and vertical diffusion. Details about the impacts of BVOCs in different PRD
cities are listed in Table 5.

We can see that surface ozone increases most in Foshan and Jiangmen where sur-
face ozone is most sensitive to BVOC emissions, and the highest increment in these
two cities is 6.1 and 5.5 ppb, respectively. The ozone in Foshan is more sensitive to
the BVOCs from outside PRD and central PRD, with the highest increment at 2.0 and
2.3 ppb, respectively. The ozone in Jiangmen is more sensitive to the BVOCs from out-
side PRD and rural PRD, with the highest increment at 2.0 and 2.5 ppb, respectively.

Zhaoqing, Zhongshan, Guangzhou and Zhuhai are in areas that are moderately sen-
sitive to BVOC emissions and the highest ozone increments in these cities are 4.0, 3.8,
3.2 and 3.1 ppb, respectively. The impacts of BVOCs from these three regions in Zhao-
qing are almost the same, while the BVOCs from central PRD affect the surface ozone
more than outside and rural PRD in Zhuhai. The ozone in Zhongshan and Guangzhou
is more sensitive to the BVOCs from the outside and the central PRD.

Duanguan, Shenzhen and Huizhou are the least sensitive areas to BVOC emissions mainly because of their upwind location, and the highest ozone increment in these cities is 2.0, 1.8 and 1.3 ppb, respectively. In Huizhou, the surface ozone isn't sensitive to BVOCs emission from the central PRD.

There are two peaks in the diurnal variation of the surface ozone increment in Zhaoqing, and the smaller one shows up at mid-day while the larger one shows up in the late afternoon. Similar to the peaks at the CZ site, the peak that appears in the late afternoon in Zhaoqing is mainly related to transport. The diurnal variations of surface ozone increment in Guangzhou and Dongguan are similar to that in Zhaoqing.

4.5 Seasonal variability

A comparison experiment to investigate the impacts of seasonal variability in BVOC emissions on ozone formation was conducted for 1–9 July (referred to here as the summer case). This period is characterized by high temperature and clear sky, and no tropical storms occurred. The model simulated mean 2-m temperature, solar radiation, wind speed, and relative humidity are 28.3°, 978.8 W m^{-2}, 4.8 m s^{-1} and 79.1 %. In this case, BVOCs and isoprene emissions are 3.2 and 3.6 times higher than in November (referred to here as the autumn case).

The simulated spatial distribution of surface ozone in summer is very different from that in autumn (Figs. 11a and 4a), because of the southwest prevailing wind direction. The high values of ozone concentration are in the northern and the eastern PRD.

Similar to the situation in autumn, BVOC emissions significantly affect the daytime ozone peak in the downwind areas in summer, including Guangzhou, Dongguan, Shenzhen and Huizhou (Fig. 11b). The maximum hourly impacts on the daytime ozone peak can be as high as 34.0 ppb over the PRD region in summer, and the maximum hourly impacts are greater in the northeast of Guangzhou (Fig. 7b). In the central area of Guangzhou-Foshan, BVOC emissions cause an average increase of surface ozone up to 9.8 ppb at 15:00:00 LT in summer and the maximum hourly impact at 15:00:00 LT in summer is 19.4 ppb.

Fig. 12 shows the comparison of the impacts of BVOCs on surface ozone in PRD cities in different seasons. The comparison reveals that the ranking of BVOC sensitive areas changes in summer. Guangzhou becomes the most sensitive area to BVOC emissions, followed by Huizhou, Dongguan, Foshan, Shenzhen, Zhenshan, Zhaoqing,
5 Zhuhai and Jiangmen. The highest surface ozone increment in Guangzhou is up to 8.8 ppb, which is 5.6 ppb higher than in autumn. Jiangmen shifts to be the area where surface ozone is the least sensitive to BVOC emissions and the highest surface ozone increment in Jiangmen is only 0.5 ppb, which is 5 ppb lower than in autumn.

There is a significant difference in the diurnal variation of the surface ozone incre-
10 ment in Zhaoqing. There are two peaks in the diurnal variation of the surface ozone increment in summer in Zhaoqing, but the larger one shifts to occur at mid-day while the smaller one shifts to occur in late afternoon. The transport influence in Zhaoqing is weaker, because it is in the upwind area in summer. So the shift indicates that not only the transport but also other factors, such as PBL compression, caused the peak in late
15 afternoon in autumn in Zhaoqing. There is a peak in the surface ozone increment in the diurnal variations in Guangzhou and in Huizhou in summer, which is related to the influence of transport and the accumulation caused by the decreasing PBL height.

In both autumn and summer seasons, the impacts of BVOC emissions on surface ozone in Guangzhou are distinct and there is a strong seasonal variation of the impacts
20 in this city. Guangzhou is the capital of Guangdong province as well as the economic, transportation and cultural center in the PRD which makes it a key target for ozone reduction strategies. However, it should be noted that strategies for solving ozone problems at this location will likely be different from those for other locations and the different season and impacts of BVOC emissions on surface ozone should be taken into account
25 when developing ozone control policies in this city.

4.6 Sensitivity of surface ozone to BVOC emissions model driving variables

Landcover, emission factors, and meteorological parameters are important drivers of MEGAN calculations, and their variations can impact the estimate of BVOC emissions

Title Page

Abstract   Introduction

Conclusions   References

Tables   Figures

◄   ►|

◄   ►

Back   Close

Full Screen / Esc

Printer-friendly Version

Interactive Discussion

(Wang et al., 2011; Fu et al., 2012) and then further influence the ozone concentration in numerical simulation. In this section, 3 experiments were performed to assess the sensitivity of surface ozone to the MEGAN drivers in November.

4.6.1 Landcover

Eucalyptus is an important BVOC emitter, because it has high terpenoid (including isoprene, monoterpene and sesquiterpene) emissions. Moreover, eucalyptus is a dominant tree in Guangdong province and is being planted widely in the PRD region because of its high economic value. We conducted a landcover change sensitivity study by changing all forest to eucalyptus, except for protected areas in national and local natural parks. The eucalyptus BVOC emission factors were adopted including an isoprene emission factor of $24\,000\,\mu g\,m^{-2}\,h^{-1}$, ~ 2 times higher than that used in the control run.

The results show that changing forests to eucalyptus increase total BVOC emissions by $\sim 23\,\%$ in PRD and isoprene emissions by $\sim 315\,\%$. Compared to the control run, there is 4.1 ppb daytime ozone peak increase due to the increase in BVOC emissions. Thus, landcover change can enhance the impacts of BVOC emissions on daytime ozone peak by 5.4 ppb over the PRD region.

The sensitivity of surface ozone at four monitoring sites at 15:00:00 LT was examined The result shows that surface ozone at CZ site has the highest responds to the BVOCs increase, followed by LH, JGW and WQS. The change of relative ranking is mainly due to the increase of BVOC emissions and the changing in spatial distribution.

4.6.2 Emission factor

BVOC emission factors dominate the total uncertainties in BVOC emission estimates which are about a factor of 3 (Lamb et al., 1987). Thus, we changed the emission factors by a factor of 3 to assess the sensitivity of surface ozone to emission factors and examine the impact of this uncertainty on surface ozone. The changes of emission

factors lead to BVOC emissions that are 200 % higher (−66.7 % lower) than that in the control run.

The daytime ozone peak is 1.3 ppb higher (0.8 ppb lower) than that in the control run. The impacts of BVOC emissions on daytime ozone peak change were between 0.5 ppb and 2.6 ppb when averaged over the PRD region.

4.6.3 Meteorology

Solar radiation and temperature are the most important meteorological parameters influencing BVOC emissions. Hence, we perturbed temperature and daytime solar radiation by their RMSE (Table 4) for each time step of the MEGAN calculations for temperature and only in daytime for solar radiation.

$$\text{SWDWON} = \text{control}_{swdown} \pm \text{RMSE}_{swdown} \tag{3}$$
$$\text{TEMP} = \text{control}_{TEMP} \pm \text{RMSE}_{TEMP} \tag{4}$$

As expected, increasing (decreasing) solar radiation and temperature produces more (less) BVOC emissions. BVOC emissions varied between −11.9 and 29.9 % due to solar radiation perturbation, and led to 0.2 ppb lower and 0.2 ppb higher daytime ozone peak in the PRD region. Thus, the impacts of BVOC emissions on the daytime ozone peak varied between 1.1 ppb and 1.5 ppb.

Similarly, there is 35.2 % increment (10.6 % decrement) of BVOC emissions due to temperature increasing (decreasing) resulting in 0.5 ppb higher (0.4 ppb lower) surface ozone. The impacts of BVOC emissions on the daytime ozone peak varied between 1.1 ppb and 1.6 ppb.

5 Conclusions

The WRF-Chem version 3.2.1 and MEGAN version 2.1 were used to estimate the impacts of BVOC emissions on surface ozone in November 2010 in the PRD region China.

⁵   The results show that there is no strong spatiotemporal variation of background surface ozone in PRD, which is related to BVOC emissions only. The daily averaged value of this background ozone concentration is ~ 25 ppb. However, the surface ozone concentration increases significantly when anthropogenic and biogenic emissions are considered, and the regional surface ozone average reaches the maximum at 15:00:00 LT
¹⁰ with the peak value of ~ 50 ppb. There is an average of ~ 3 ppb surface ozone associated with BVOC emissions that contribute to the daytime ozone peak and the maximum hourly impacts of BVOC emissions on the daytime ozone peak is 24.8 ppb. As the most abundant non-methane BVOC species, isoprene contributes ~ 57 % of the impacts of BVOC emissions on daytime ozone peak. BVOCs have the greatest impact on daytime
¹⁵ ozone peak in urban and downwind areas, especially the central area of Guangzhou-Foshan and the western Jiangmen.

    The impact pattern of BVOC emissions on surface ozone is strongly related to weather conditions, especially the wind speed and wind direction. Three conditions are classified based on wind conditions, and the possibility of their occurrence is 60 %,
²⁰ 36.7 % and 3.3 %, respectively. The condition of calm winds is of particular interest because BVOC emissions can affect the daytime ozone peak widely and significantly in the PRD region.

    Impacts of BVOCs from three regions in the modeling domain on surface ozone have been estimated, and the BVOCs from the outside and the central PRD affect
²⁵ the surface ozone in the central area of Guangzhou-Foshan more than the BVOCs from the rural PRD. BVOCs from the rural PRD affect the surface ozone in western Jiangmen significantly. Among PRD cities, Foshan and Jiangmen are where surface

ozone is most sensitive to BVOC emissions, with the highest concentration increment of 6.0 ppb and 5.5 ppb.

There is strong seasonal variation of impacts of BVOC emissions on surface ozone, and the most sensitive areas of surface ozone to BVOC emissions shift to be Guangzhou and Huizhou in summer. Guangzhou is a place where surface ozone is very sensitive to BVOC emissions in both autumn and summer, so the strategies for solving ozone problems for this city will likely be different and the impacts of BVOC emissions should be considered when developing ozone control policies in this location.

Sensitivity experiments indicate that surface ozone responds differently to various MEGAN drivers. Related to the amount and spatial distribution of BVOC emissions, landcover is the most important MEGAN driver to which the sensitivity of surface ozone is the highest. Emission factors are another MEGAN factor to which surface ozone is very sensitive. Under the current BVOCs spatial distribution, ozone in the urban area is more sensitive to BVOC emission changes.

This study presents initial results indicating that BVOC emissions can affect surface ozone significantly in the PRD region and that the impacts are complex Further work will quantitatively investigate the chemical, biological and physical processes that control the impact of BVOC emissions on surface ozone in the PRD region. Moreover, more work will be done to improve the emission factors of BVOCs in the PRD region since the BVOC emission factors used in this study are very uncertain.

References

Adams, R. P.: Identification of essential oil components by gas chromatography/mass spectrometry quadrupole, Allured Publ. Corp., Carol Stream, 2001.

Atkinson, R. and Arey, J.: Atmospheric degradation of Volatile Organic Compounds, Chem. Rev., 103, 4605–4638, 2003.

Bai, J. H. and Wang, X. M.: A study of nonmethane hydrocarbons at subtropical forest Part I: Seasonal variation (flask sampling), China Clim. Environ. Res., 6, 286–293, 2001a.

Bai, J. H. and Wang, X. M.: A study of nonmethane hydrocarbons at subtropical forest Part II: Diurnal variation, China Clim. Environ. Res., 6, 456–466, 2001b.

Baker, B., Guenther, A., and Greenberg, J.: Canopy level fluxes of 2-methyl-3buten-2-ol, acetone, and methanol by a portable relaxed eddy accumulation system, Environ. Sci. Technol., 35, 1707–1708, 2001.

Barkley, M. P., Palmer, P. I., Smedt, I. D., Karl, T., Guenther, A., and Roozendael, M. V.: Regulated large-scale annual shutdown of Amazonian isoprene emissions?, Geophys. Res. Lett., 36, L04803, doi:10.1029/2008GL036843, 2009.

Bao, H., Shrestha, K. L., Kondo, A., Kaga, A., Inoue, Y.: Modeling the influence of biogenic volatile organic compound emissions on ozone concentration during summer season in the Kinki region of Japan, Atmos. Environ., 44, 421–431, 2009.

Bonan, G. B., Levis, S., Kergoat, L., and Oleson, K. W.: Landscapes as patches of plant functional types: an integrating concept for climate and ecosystem models, Global Biogeochem. Cy., 16, 1021, doi:10.1029/2000GB001360, 2000.

Bowling, D. R., Turnipseed, A. A., Delany, A. C., Baldocchi, D. D., Greenberg, J. P., and Monson, R. K.: The use of relaxed eddy accumulation to measure biosphere-atmosphere exchange of isoprene and other biological trace gased, Oecologia, 116, 306–315, 1998.

Businger, J. A. and Oncley, S. P.: Flux measurement with conditional sampling, Note. Correspond., 7, 349–352, 1990.

Carslaw, N., Bell, N., Lewis, A. C., McQuaid, J. B., and Pilling, M. J.: A detailed case study of isoprene chemistry during the EASE96 Mace Head campaign, Atmos. Environ., 34, 2827–2836, 2000.

Chameides, W. L., Fehsenfeld, F., Rodgers, M. O., Cardelino, C., Martinez, J., Parrish, D., Lonneman, W., Lawson, D. R., Rasmussen, R. A., Zimmerman, P., and Greenberg, J.: Ozone precursor relationships in the bmbient atmosphere, J. Geophys. Res., 97, 6037–6055, 1992.

Title Page

Abstract | Introduction

Conclusions | References

Tables | Figures

|◄ | ►|

◄ | ►

Back | Close

Full Screen / Esc

Printer-friendly Version

Interactive Discussion

Chen, F. and Dudhia, J.: Coupling an advanced land surface-hydrology model with the Penn State-NCAR MM5 modeling system. Part I: Model implementation and sensitivity, Mon. Weather Rev., 129, 569–585, 2001.

Cheng, H. R., Guo, H., Wang, X. M., Saunders, S. M., Lam, S. H. M., Jiang, F., Wang, T. J., Ding, A. J., Lee, S. C., and Ho, K. F.: On the relationship between ozone and its precursors in the Pearl River Delta: application of an observation-based model (OBM), Environ. Sci. Pollut. Res., 17, 547–560, doi:10.1007/s11356-009-0247-9, 2010.

Chou, M. D., Suarez, M. J., Ho, C. H., Yan, M.H H., and Lee, K. T.: Parameterizations for cloud overlapping and shortwave single-scattering properties for use in general circulation and cloud ensemble models, J. Climate, 11, 202–214, 1998.

Collins, W. J., Derwent, R. G., Johnson, C. E., and Stevenson, D. S.: The oxidation of organic compounds in the troposphere and their global warming potentials, Climatic Change, 52, 453–479, 2002.

Curci, G., Beekmann, M., Vautard, R., Smiatek, G., Steinbrecher, R., Theloke, J., and Friedrich, R.: Modelling study of the impact of isoprene and terpene biogenic emissions on European ozone levels, Atmos. Environ., 43, 1444–1455, 2009.

Deng, A. J., Stauffer, D. R., Dudhia, J., Otte, T., and Hunter, G. K.: Update analysis nudging FDDA in WRF-ARW, The 8th WRF Users'sWorkshop, 11–15 June, Boulder, CO, available at: http://www.mmm.ucar.edu/wrf/users/workshops/WS2007/abstracts/4-8_Deng.pdf, 2007.

Fabien, S., Sarrat, C., Serca, D., Tulet, P., and Rosset, R.: Isoprene and monoterpenes biogenic emissions in France: modeling and impact during a regional pollution episode, Atmos. Environ., 38, 3853–3865, 2004.

Fan, S. J., Wang, B. M., Tesche, M., Engelmann, R., Althausen, A., Liu, J., Zhu, W., Fan, Q., Li, M. H., Ta, N., Song, L. L., and Leong, K.: Meteorological conditions and structures of atmospheric boundary layer in October 2004 over Pearl River Delta area, Atmos. Environ., 42, 6174–6186, 2008.

Fast, J. D., Gustafson, Jr., Easter, W. I., Zaveri, R. C., Barnard, J. C., Chapman, E. G., Grell, G. A., and Packham, S. E.: Evolution of ozone, particulates and aerosol direct radiative forcing in the vicinity of Houston using a fully coupled meteorology-chemistry-aerosol model, J. Geophys. Res., 111, D21305, doi:10.1029/2005JD006721, 2006.

Fu, Y. and Liao, H.: Simulation of the interannual variations of biogenic emissions of volatile organic compounds in China: impacts on tropospheric ozone and secondary organic aerosol, Atmos. Environ., 59, 170–185, 2012.

Title Page

Abstract | Introduction

Conclusions | References

Tables | Figures

◀ | ▶

◀ | ▶

Back | Close

Full Screen / Esc

Printer-friendly Version

Interactive Discussion

Geng, F., Tie, X., Guenther, A., Li, G., Cao, J., and Harley, P.: Effect of isoprene emissions from major forests on ozone formation in the city of Shanghai, China, Atmos. Chem. Phys., 11, 10449–10459, doi:10.5194/acp-11-10449-2011, 2011.

Granier, C., Petron, G., Muller, J. F., and Brasseur, G.: The impact of natural and anthropogenic hydrocarbons on the tropospheric budget of carbon monoxide, Atmos. Environ., 34, 5255–5270, 2000.

Grell, G. A., Peckham, S. E., Schmitz, R., McKeen, S. A., Frost, G., Skamarock, W. C., and Eder, B.: Fully coupled "online" chemistry within the WRF model, Atmos. Environ., 39, 6957–6975, 2005.

Guenther, A., Hewitt, C. N., Erickson, D., Fall, R., Geron, C., Graedel, T., Harley, P., Klinger, L., Lerdau, M., McKay, W. A., Pierce, T., Scholes, B., Steinbrecher, R., Tallamraju, R., Taylor, J., and Aimmerman, P.: A global model of natural volatile organic compound emissions, J. Geophys. Res., 100, 8873–8892, 1995.

Guenther, A., Baugh, W., Davis, K., Hampton, G., Harley, P., Klinger, L., Vierling, L., and Zimmerman, P.: Isoprene fluxes measured by enclosure, relaxed eddy accumulation, surface layer gradient, mixed layer gradient, and mixed layer mass balance techniques, J. Geophys. Res., 101, 18555–18567, 1996a.

Guenther, A., Zimmerman, P., Klinger, L., Greenberg, J., Ennis, C., Davis, K., and Pollock, W.: Estimates of regional natural volatile organic compound fluxes from enclosure and ambient measurements, J. Geophys. Res., 101, 1345–1359, 1996b.

Guenther, A., Baugh, B., Brasseur, G., Greenberg, J., Harley, P., Klinger, L., Serca, D., and Vierling, L.: Isoprene emission estimates and uncertainties for the central african espresso study domain, J. Geophys. Res., 104, 30625–30639, 1999.

Guenther, A., Karl, T., Harley, P., Wiedinmyer, C., Palmer, P. I., and Geron, C.: Estimates of global terrestrial isoprene emissions using MEGAN (Model of Emissions of Gases and Aerosols from Nature), Atmos. Chem. Phys., 6, 3181-3210, doi:10.5194/acp-6-3181-2006, 2006.

Guenther, A. B., Jiang, X., Heald, C. L., Sakulyanontvittaya, T., Duhl, T., Emmons, L. K., and Wang, X.: The Model of Emissions of Gases and Aerosols from Nature version 2.1 (MEGAN2.1): an extended and updated framework for modeling biogenic emissions, Geosci. Model Dev., 5, 1471–1492, doi:10.5194/gmd-5-1471-2012, 2012.

Title Page

Abstract | Introduction

Conclusions | References

Tables | Figures

|◄ | ►|

◄ | ►

Back | Close

Full Screen / Esc

Printer-friendly Version

Interactive Discussion

Hoffmann, T., Odum, J. R., Bowman, F., Collins, D., Klockow, D., Flagan, R. C., and Seinfeld, J. H.: Formation of organic aerosols from the oxidation of biogenic hydrocarbons, J. Atmos. Chem., 26, 189–222, 1997.

Janjic, Z. L.: Nonsingular Implementation of the Mellor-Yamada Level 2.5 Scheme in the NCEP Meso model, NCEP Office Note, 437: 61, 2002.

Kain, J. S. and Fritsch, J. M.: A one-dimensional entraining/detraining plume model and its application in convective parameterization, J. Atmos. Sci., 47, 2784–2802, 1990.

Kain, J. S. and Fritsch, J. M.: Convective parameterization for mesoscale model: the Kain–Fritsch scheme. The representation of cumulus convection in numerical model, Meteor. Monogr., No. 24, Amer. Meteor. Soc., 165–170, 1993.

Klinger, L. F., Li, Q. J., Guenther, A., Greenberg, J., Baker, B., and Bai, J. H.: Assessment of volatile organic compound emissions from ecosystems of China, J. Geophys. Res., 107, ACH 16–19, 2002.

Lamb, B., Guenther, A., Gay, D., and Westberg, H.: A national inventory of biogenic hydrocarbon emissions, Atmos. Environ., 21, 1695–1705, 1987.

Li, G. H., Zhang, R. Y., Fan, J. W., and Tie, X. X.: Impacts of biogenic emissions on photochemical ozone production in Houston, Texas, J. Geophys. Res., 112, D10309, doi:10.1029/2006JD007924, 2007.

Li, Y.: Numerical Studies on Ozone Source Apportionment and Formation Regime and their Implications on Control Strategies, Ph.D. thesis, Hong Kong University of Science and Technology, Hongkong, 2011.

Lin, Y. L., Farley, R. D., and Orvilie, H. D.: Bulk parameterization of the snow field in a cloud model, J. Clim. Appl. Meteorol., 22, 1065–1092, 1983.

Lu, K. D., Rohrer, F., Holland, F., Fuchs, H., Bohn, B., Brauers, T., Chang, C. C., Häseler, R., Hu, M., Kita, K., Kondo, Y., Li, X., Lou, S. R., Nehr, S., Shao, M., Zeng, L. M., Wahner, A., Zhang, Y. H., and Hofzumahaus, A.: Observation and modelling of OH and HO_2 concentrations in the Pearl River Delta 2006: a missing OH source in a VOC rich atmosphere, Atmos. Chem. Phys., 12, 1541–1569, doi:10.5194/acp-12-1541-2012, 2012.

Marley, N. A., Gaffney, J. S., Tackett, M., Sturchio, N. C., Heraty, L., Martinez, N., Hardy, K. D., Marchany-Rivera, A., Guilderson, T., MacMillan, A., and Steelman, K.: The impact of biogenic carbon sources on aerosol absorption in Mexico City, Atmos. Chem. Phys., 9, 1537–1549, doi:10.5194/acp-9-1537-2009, 2009.

Martilli, A., Clappier, A., and Rotach, M. W.: An urban surface exchange parameterization for mesoscale models, Bound.-Lay. Meteorol., 104, 261–304, 2002.

Mass, C. and Ovens, D.: Wrf Model Physics: Problems, Solutions and a New Paradigm for Progress, Preprints, WRF Users' Workshop, Boulder, CO, NCAR, 2010.

Mass, C. and Ovens, D.: Fixing WRF's high speed wind bias: a new subgrid scale drag parameterization and the role of detailed verification, Preprints, 24th Conf. on Weather and Forecasting/20th Conf. on Numerical Weather Prediction, Seattle, WA, Amer. Meteor. Soc., 9B.6, 2011.

Mlawer, E. J., Taubman, S. J., Brown, P. D., Iacono, M. J., and Clough, S. A.: Radiative transfer for inhomogeneous atmosphere: RRTM, a validated correlated-K model for longwave, J. Geophys. Res., 102, 16663–16682, 1997.

Monson, R. K., Harley, P. C., Litvak, M. E., Wildermuth, M., Guenther, A. B., Zimmerman, P. R., and Fall, R.: Environmental and developmental controls over the seasonal pattern of isoprene emission from aspen leaves, Oecologia, 99, 260–270, 1994.

Oleson, K. W. and Bonan, G. B.: The effects of remotely sensed plant functional type and Leaf Area Index on simulations of boreal forest surface fluxes by the NCAR Land Surface Model, J. Hydrometeorol., 1, 431–446, 2000.

Petron, G., Harley, P., Greenberg, J., and Guenther, A.: Seasonal temperature variations influence isoprene emission, Geophys. Res. Lett., 28, 1707–1710, 2001.

Pierce, T., Geron, C., Bender, L., Dennis, R., Tonnesen, G., and Guenther, A.: Influence of increased isoprene emissions on regional ozone modeling, J. Geophys, Res.-Atmos., 103, 25611–25629, 1998.

Poisson, N., Kanakidou, M., and Crutzen, P. J.: Impact of non-methane hydrocarbons on tropospheric chemistry and the oxidizing power of the global troposphere: 3-dimensional modeling results, J. Atmos. Chem., 36, 157–230, 2000.

Roux, G., Liu, Y., Monache, L. D., Sheu, R.-S., and Warner, T. T.: Verification of high resolution WRF-RTFDDA surface forecasts over mountains and plains, Preprints, WRF Users' Workshop, Boulder, CO, NCAR, 2009.

Sakulyanontvittaya, T., Duhl, T., Wiedinmyer, C., Helmig, D., Matsunaga, S., Potosnak, M., Milford, J., and Guenther, A.: Monoterpene and sesquiterpene emission estimates for the United States, Environ. Sci. Technol., 42, 1623–1629, 2008.

Title Page

Abstract | Introduction

Conclusions | References

Tables | Figures

|◄ | ►|

◄ | ►

Back | Close

Full Screen / Esc

Printer-friendly Version

Interactive Discussion

Sanderson, M. G., Jones, C. D., Collins, W. J., Johnson, C. E., and Derwent, R. G.: Effect of climate change on isoprene emissions and surface ozone levels, Geophys. Res. Lett., 30, 1936, doi:10.1029/2003GL017642, 2003.

Skamarock, W. C., Klemp, J. B., Dudhia, J., Gill, D. O., Barker, D. M., Duda, M. G., Huang, X. Y., Wang, W., and Powers, J. G.: A Description of the Advanced Research WRF Version 3, Technical Report, National Center for Atmospheric Research, TN-475, +STR, 2008.

Tang, J. H., Chan, L. Y., Chan, C. Y., Li, Y. S., Chang, C. C., Liu, S. C., Wu, D., and Li, Y. D.: Characteristics and diurnal variations of NMHCs at urban, suburban, and rural sites in the Pearl River Delta and a remote site in South China, Atmos. Environ., 41, 8620–8632, 2007.

Thunis, P. and Cuvelier, C.: Impact of biogenic emissions on ozone formation in the Mediterranean area – a BEMA modeling study, Atmos. Environ., 34, 467–481, 2000.

Tsui, J., Guenther, A., Yip, W. K., and Chen, F.: A biogenic volatile organic compound emission inventory for Hong Kong, Atmos. Environ., 43, 6442–6448, doi:10.1016/j.atmosenv.2008.01.027, 2009.

Viney, P. A., Yoder, G. T., and Arya, S. P.: Ozone in the urban southeastern United States, Environ. Pollut., 75, 39–44, 1992.

Wang, X., Zhang, Y., Hu, Y., Zhou, W., Lu, K., Zhong, L., Zeng, L., Shao, M., Hu, M., and Russell, A. G.: Process analysis and sensitivity study of regional ozone formation over the Pearl River Delta, China, during the PRIDE-PRD2004 campaign using the Community Multiscale Air Quality modeling system, Atmos. Chem. Phys., 10, 4423–4437, doi:10.5194/acp-10-4423-2010, 2010.

Wang, X. M., Carmichael, G., Chen, D. L., Tang, Y. H., and Wang, T. J.: Impacts on different emission sources on air quality during March 2001 in the Pearl River Delta (PRD) region, Atmos. Environ., 39, 5227–5241, 2005.

Wang, X. M., Lin, W. S., Yang, L. M., Deng, R.R., and Lin, H.: A numerical study of influences of urban land-use change on ozone distribution over the Pearl River Delta Region, China, Tellus B, 59, 633–641, 2007.

Wang, X. M., Chen, F., Wu, Z. Y., Zhang, M. G., Tewari, M., Guenther, A., and Wiedinmyer, C.: Impacts of weather conditions modified by urban expansion on surface ozone: comparison between the Pearl River Delta and Yangtze River Delta regions, Adv. Atmos. Sci., 26, 962–972, 2009.

Wang, X. M., Situ, S. P., Guenther, A., Chen, F., Wu, Z. Y., Xia, B. C., and Wang, T. J.: Spatiotemporal variability of biogenic terpenoid emissions in Pearl River Delta, China, with high-resolution land-cover and meteorological data, Tellus B, 63, 241–254, 2011.

Wei, X. L., Li, Y. S., Lam, K. S., Wang, A. Y., and Wang, T. J.: Impact of biogenic VOC emissions on a tropical cyclone-related ozone episode in the Pearl River Delta region, China, Atmos. Environ., 41, 7851–7861, 2007.

Zaveri, R. Z. and Peters, L. K.: A new lumped structure photochemical mechanism for long-scale applications, J. Geophys. Res., 104, 30387–30414, 1999.

Zaveri, R. A., Easter, R. C., Fast, J. D., and Peters, L. K.: Model for Simulating Aerosol Interactions and Chemistry (MOSAIC), J. Geophys. Res., 113, D13204, doi:10.1029/2007JD008782, 2008.

Zhang, Y. H., Su, H., Zhong, L. J., Cheng, Y. F., Zeng, L. M., Wang, X. S., Xiang, Y. R., Wang, J. L., Gao, D. F., Shao, M., and Liu, S. C.: Regional ozone pollution and observation-based approach for analyzing ozone-precursor relationship during the PRIDE-PRD2004 campaign, Atmos. Environ., 42, 6203–6218, 2008.

Zheng, J. Y., Zhang, L. J., Che, W. W., Zheng, Z. Y., and Yin, S. S.: A highly resolved temporal and spatial air pollutant emission inventory for the Pearl River Delta region, China and its uncertainty assessment, Atmos. Environ., 43, 5112–5122, 2009.

Zheng, J. Y., Zhong, L. J., Wang, T., Louie, P. K. K., and Li, Z. C.: Ground-level ozone in the Pearl River Delta region: analysis of data from a recently established regional air quality monitoring network, Atmos. Environ., 44, 814–823, 2010a.

Zheng, J. Y., Zheng, Z. Y., Yu, Y. F., and Zhong, L. J.: Temporal, spatial characteristics and uncertainty of biogenic VOC emissions in the Pearl River Delta area, Atmos. Environ., 44, 1960–1969, 2010b.

Zhou, G. Y., Guan, L. L., Wei, X. H., Zhang, D. Q., Zhang, Q. M., Yan, J. H., Wen, D. Z., Liu, J. X., Liu, S. G., Huang, Z. L., Kong, G. H., Mo, J. M., and Yu, Q. F.: Litterfall production along successional and altitudinal gradients of subtropical monsoon evergreen broadleaved forests in Guangdong, China, Plant Ecol., 188, 77–89, 2007.

Title Page

Abstract | Introduction

Conclusions | References

Tables | Figures

|◄ | ►|

◄ | ►

Back | Close

Full Screen / Esc

Printer-friendly Version

Interactive Discussion

Table 1. WRF-Chem configuration.

Process	WRF-Chem option
Microphysics	Lin
Long-wave radiation	RRTM
Short-wave radiation	Goddard
Surface layer	Monin–Obukhov (Janjic) scheme
Land surface model	Noah LSM
Urban canopy model	Multi-layer, Building Environment Parameterization (BEP) scheme
Boundary layer scheme	Mellor–Yamada–Janjic TKE scheme
Cumulus parameterization	Kain–Fritsch (new Eta) parameterization scheme
Photolysis scheme	Fast-J
Gas-phase mechanism	CBM-Z
Aerosol model	MOSAIC

Table 2. General meteorological conditions including surface pressure, temperature, wind speed and relative humidity during simulated period.

	Pressure (hPa)	Temperature (˚C)	Wind speed (m s^{-1})	Relative humidity (%)
Mean	1011.9	19.5	1.8	66.0
Maximum	1018.4	23.7	4.7	91.0
Minimum	1000.8	15.0	0.4	40.0

Table 3. Description of model simulations.

Simulation	Anthropogenic emissions	Biogenic VOCs emissions
Control	All anthropogenic emissions	All BVOCs
Case 1	No anthropogenic emissions	All BVOCs
Case 2	All anthropogenic emissions	No BVOCs
Case 3	All anthropogenic emissions	No isoprene
Case 4	All anthropogenic emissions	No BVOCs in outside PRD
Case 5	All anthropogenic emissions	No BVOCs in rural PRD
Case 6	All anthropogenic emissions	All BVOCs in 1–9 Jul
	No anthropogenic emissions	All BVOCs in 1–9 Jul

Table 4. Verification statistics of meteorological simulations.

Meteorological variable	Num	MEAN		Bias	MAE	RMSE
		Obs	Sim			
SWDOWN ($\mathrm{W\,m^{-2}}$)	1	163.8	229.8	64.2	82.9	152.0
2-m TEMP (°C)	9	19.5	20.7	1.2	1.4	1.6
10-m WSPD ($\mathrm{m\,s^{-1}}$)	9	1.8	3.9	2.2	2.2	2.4
2-m RH (%)	9	66.3	64.2	−2.1	8.5	8.5

SWDOWN: downward shortwave radiation;
2-m TEMP: temperature at 2 m;
Obs: observation;
Sim: simulation;
MAE: mean absolute error;
RMSE: root mean square error;
Num: number of stations.

Table 5. The maximum impacts of BVOCs emissions on surface ozone in the PRD cities and the contribution from different regions (unit: ppb).

	FS	JM	ZQ	ZS	GZ	ZH	DG	SZ	HZ
Impacts	6.1	5.5	4.0	3.8	3.2	3.1	2.0	1.8	1.3
Outside	2.0	2.0	1.2	1.2	1.1	0.9	1.0	0.6	0.7
Rural	1.8	2.5	1.4	0.9	0.7	0.6	0.7	0.7	0.5
Central	2.3	1.0	1.4	1.7	1.4	1.6	0.3	0.5	0.1

Outside: impacts of BVOCs from the outside PRD;
Rural: impacts of BVOCs from the rural PRD;
Central: impacts of BVOCs from the central PRD.
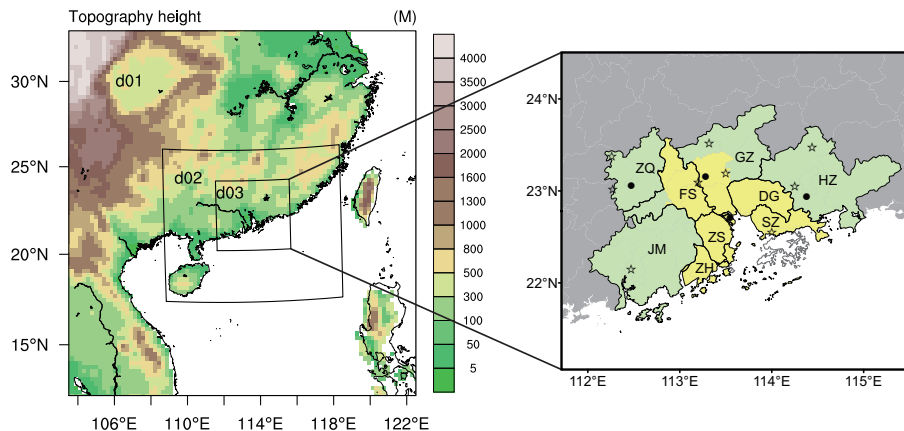
Fig. 1. Modeling domains topography, location of meteorological monitoring sites (star) and air quality monitoring sites (filled circle). Definition of the three regions: grey area is the outside PRD; green area is the rural PRD; yellow area is the central PRD.

Fig. 2. Spatial distributions of anthropogenic and biogenic emissions flux in the Pearl River Delta (PRD) region: **(a)** sulfur dioxide; **(b)** carbon monoxide; **(c)** nitric oxide; **(d)** total anthropogenic VOCs; **(e)** total biogenic VOCs.
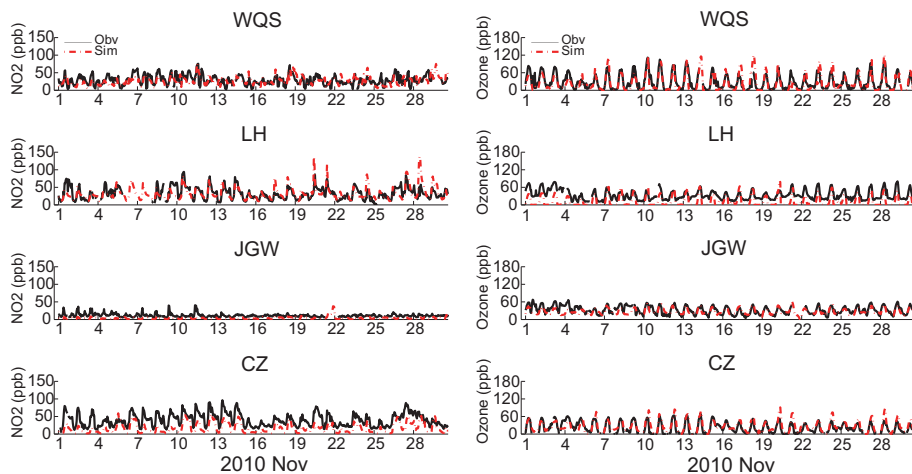
Fig. 3. The simulated and observed hourly nitrogen dioxide (NO_2) and surface ozone at 4 PRD monitoring sites in November 2010 (the location of the sites are shown in Fig. 2).
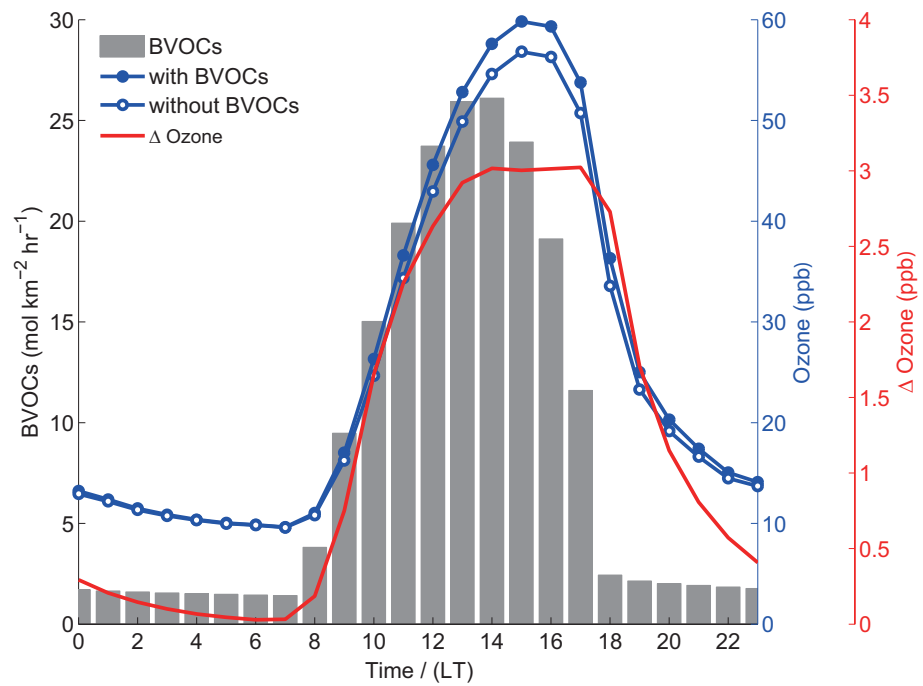
Fig. 4. Diurnal variation of total BVOCs emission rate, surface ozone concentration with and without BVOCs emissions, and their difference Δ ozone over the PRD region.
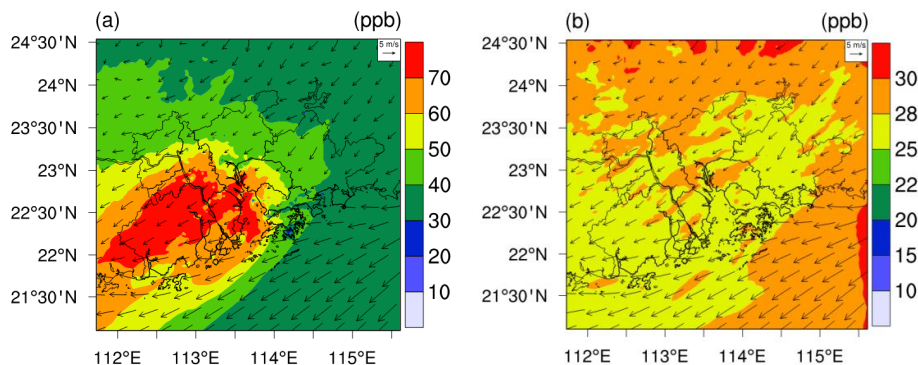
Fig. 5. Spatial distributions of surface ozone at 15:00:00 LT in **(a)** control run and **(b)** in background run.
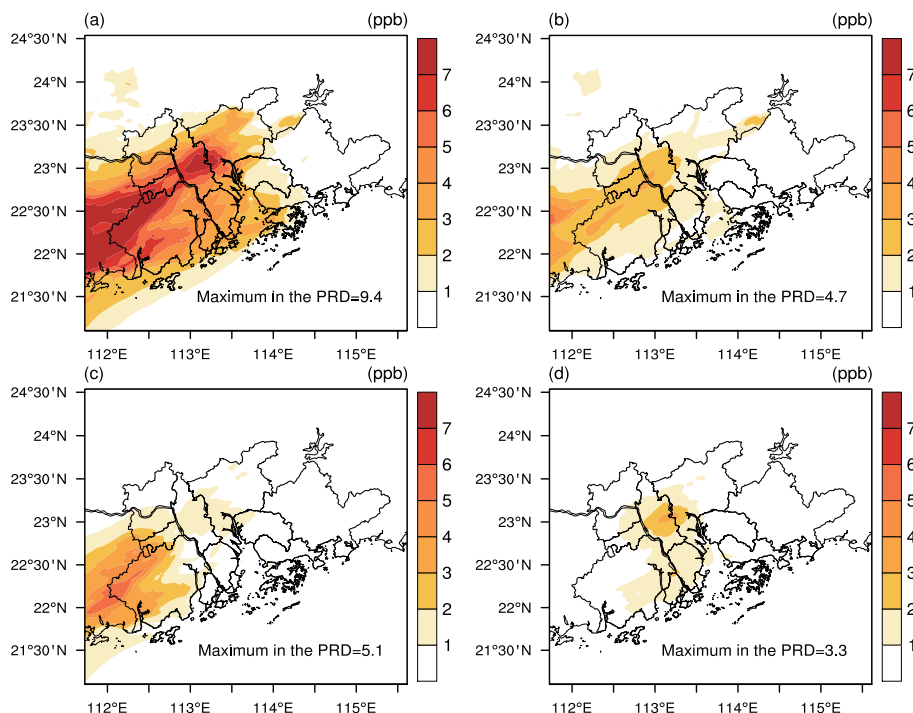
Fig. 6. Changes of the daytime ozone peak due to BVOC emissions: **(a)** spatial distribution of surface ozone changes due to BVOC emissions from the whole domain; **(b)** spatial distribution of surface ozone changes due to BVOC emissions from the outside PRD; **(c)** spatial distribution of surface ozone changes due to BVOC emissions from the rural PRD; **(d)** spatial distribution of surface ozone changes due to BVOC emissions from the central PRD.

Title Page

Abstract | Introduction

Conclusions | References

Tables | Figures

|◄ | ►|

◄ | ►

Back | Close

Full Screen / Esc

Printer-friendly Version

Interactive Discussion
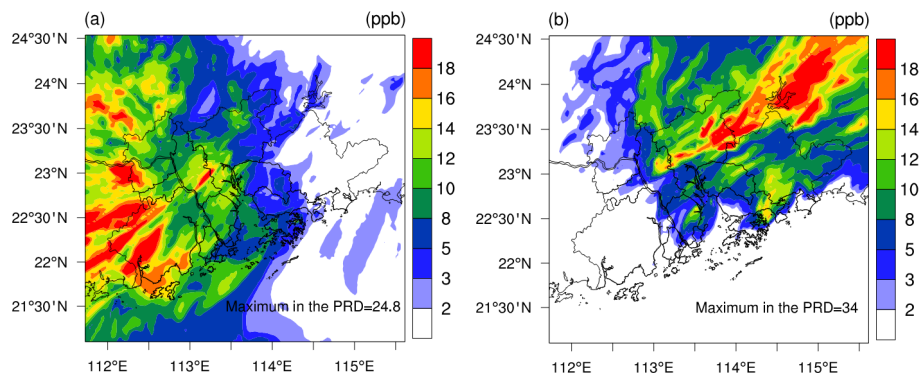
Fig. 7. Maximum hourly impacts of BVOC emissions on the daytime ozone peak **(a)** in autumn and **(b)** in summer.

Title Page

Abstract | Introduction

Conclusions | References

Tables | Figures

◄ | ►

Back | Close

Full Screen / Esc

Printer-friendly Version

Interactive Discussion
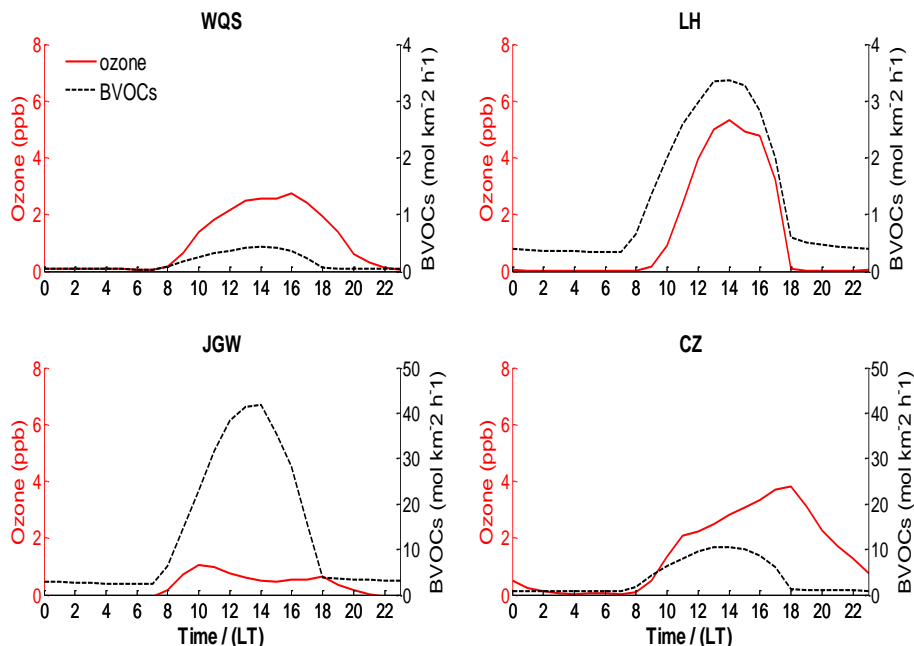
Fig. 8. Diurnal variations of modeled surface ozone changes and BVOC emission rate at 4 monitoring sites. The red dashed line shows surface ozone changes (ppb) while the black solid line shows BVOC emission rate ($mol\,km^{-2}\,h^{-1}$).
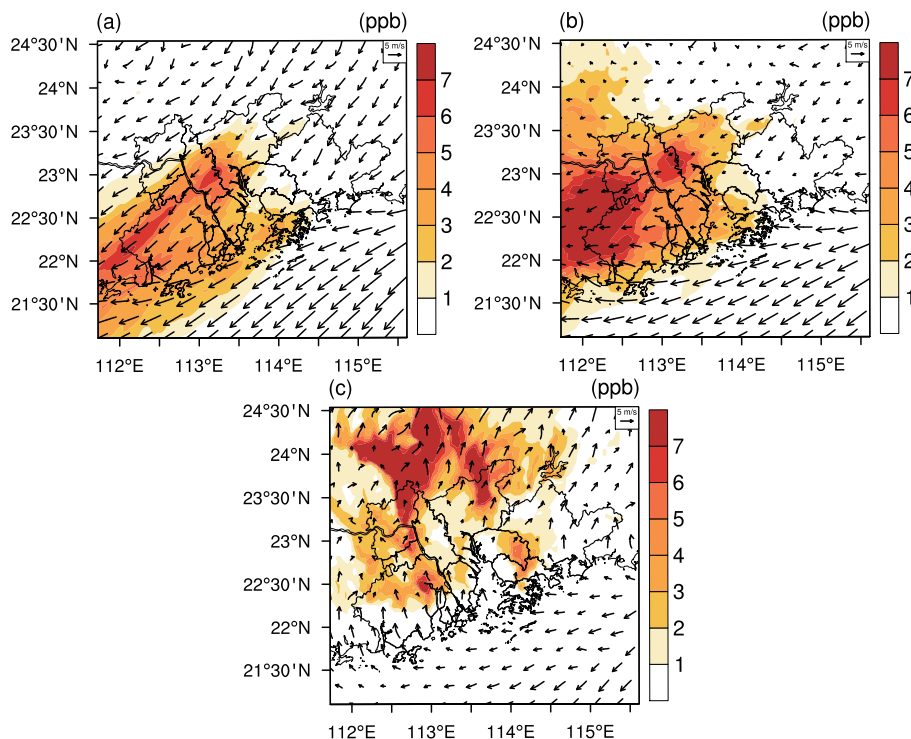
Fig. 9. Spatial distributions of the daytime ozone peak changes due to BVOC emissions under different meteorological conditions: **(a)** north wind condition; **(b)** calm wind condition; **(c)** south wind condition.
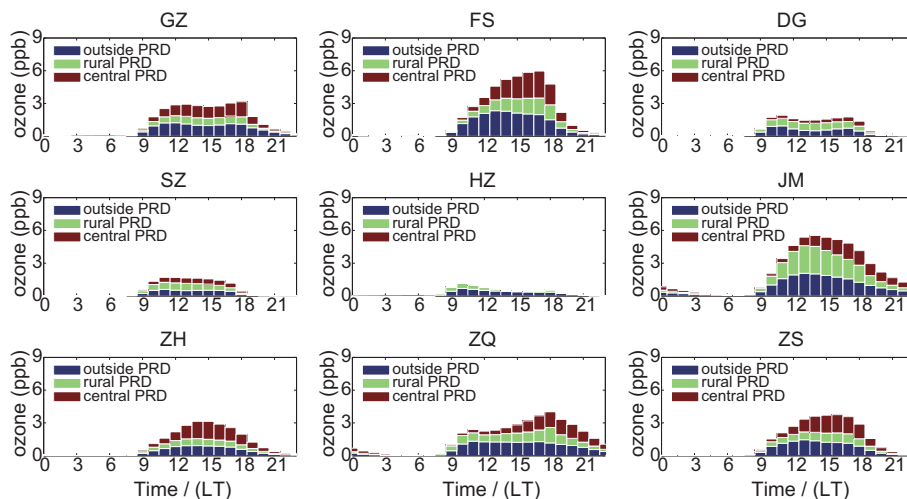
Fig. 10. Diurnal variation of the surface ozone increment in PRD cities due to BVOC emissions from different regions.

Seasonal and regional variability in biogenic VOC emissions

S. Situ et al.

Title Page

Abstract | Introduction

Conclusions | References

Tables | Figures
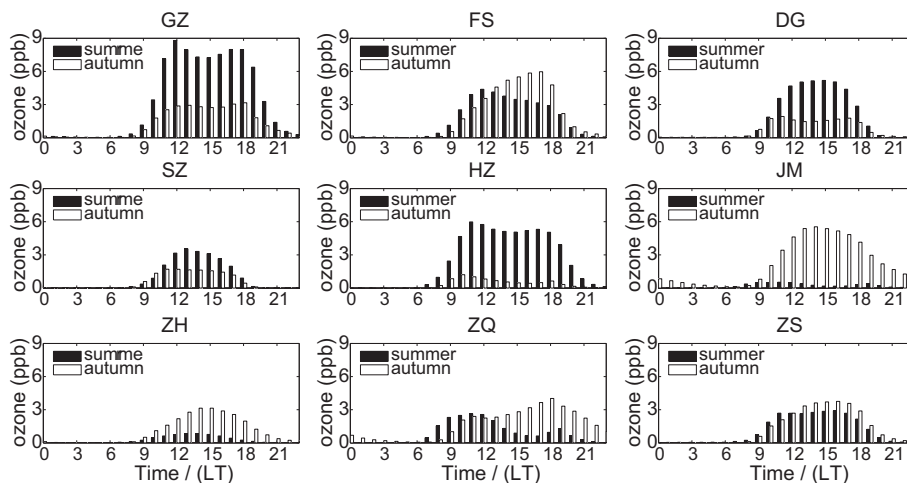
◄ | ►

Back | Close

Full Screen / Esc

Printer-friendly Version

Interactive Discussion
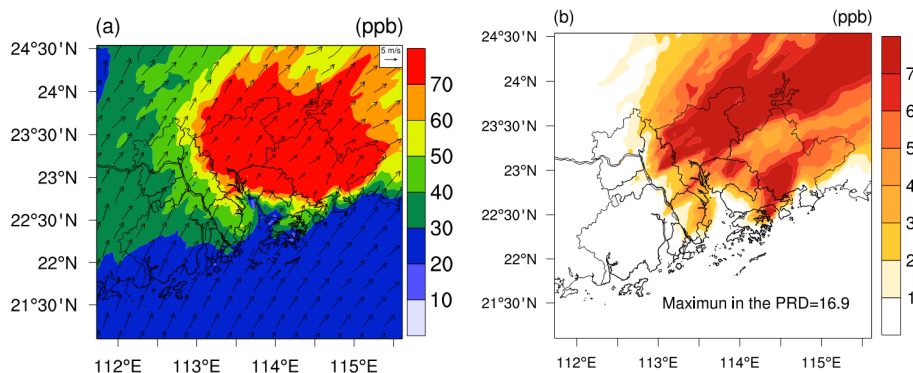
Fig. 11. Spatial distributions of **(a)** surface ozone and **(b)** the impacts of BVOC emissions on surface ozone at 15:00:00 LT in summer.

Title Page

Abstract | Introduction

Conclusions | References

Tables | Figures

◀◀ | ▶▶

◀ | ▶

Back | Close

Full Screen / Esc

Printer-friendly Version

Interactive Discussion

Fig. 12. Comparison of BVOCs impacts on surface ozone in PRD cities in summer and in autumn.